RESEARCH ARTICLE

Mathematical Modeling of Driving Forces of an Electric Vehicle for Sustainable Operation

**ANUBHAV AGRAWAL¹, RANBIR SINGH², NAGENDRA KUMAR³, VIJAY PRAKASH SINGH²,
MAJED A. ALOTAIBI⁴, HASMAT MALIK⁵,⁶, FAUSTO PEDRO GARCíA MÁRQUEZ⁷,
AND MOHAMMAD ASEF HOSSAINI⁸**

¹Department of Electronics and Communication Engineering, BML Munjal University, Gurugram 122413, India
²Department of Mechanical Engineering, BML Munjal University, Gurugram 122413, India
³Department of Electrical and Electronics Engineering, G. L. Bajaj Institute of Technology and Management, Greater Noida 201306, India
⁴Department of Electrical Engineering, College of Engineering, King Saud University, Riyadh 11421, Saudi Arabia
⁵Department of Electrical Power Engineering, Faculty of Electrical Engineering, Universiti Teknologi Malaysia (UTM), Johor Bahru 81310, Malaysia
⁶Department of Electrical Engineering, Graphic Era (Deemed to be University), Dehradun 248002, India
⁷Ingenium Research Group, Universidad Castilla-La Mancha, 13071 Ciudad Real, Spain
⁸Department of Physics, Badghis University, Badghis 3351, Afghanistan

Corresponding authors: Mohammad Asef Hossaini (asef.hossaini_edu@basu.edu.af), Majed A. Alotaibi (majedalotaibi@ksu.edu.sa), and Hasmat Malik (hasmat@utm.my)

ABSTRACT Increasing greenhouse gases & air pollution are a global threat. Global forums are aggressively emphasizing on reducing the dependence on non-renewable resources. Battery Electric vehicle are among the initial initiative to reduce dependency on fossil fuels, and this demands more research to understand the energy requirements of a vehicle under different driving conditions. The performance of an Electric Vehicle depends on varying drive conditions and the Power Electronic Controller is primarily responsible for its sustainable operation. In this paper, a novel mathematical model is proposed to analyze the performance of an electric vehicle under different driving conditions. The model is simulated at different driving speeds keeping other longitudinal, lateral, and vertical parameters fixed. Rolling resistance forces, aerodynamic drag force, gradient force, total driving force, driving torque, and power requirements at different speeds have been calculated under standard driving conditions. The rolling resistance increases by 2.16 times with a change in the vehicle speed from 40 kmph to 120 kmph. The aerodynamic drag force increases ten times with a 10-degree gradient. The battery operating temperature is critical in vehicular performance, a hybrid Pneumatic-Liquid Thermal Management System is proposed to maintain battery operating temperature. Performance of the proposed model is simulated and found to be in line with the existing standards. This study concludes that road conditions, tyre pressure, velocity of travel, wind velocity, and temperature significantly influence the performance of an electric vehicle.

INDEX TERMS Sustainability, battery electric vehicle, electric vehicle, electric vehicle modeling, rolling resistance, aerodynamic drag, energy efficiency, pneumatic thermal management system.

ABBREVIATIONS
ABBREVIATIONS USED IN THE PRESENT RESEARCH ARTICLE

m	Total mass of vehicle in kg.
g	Gravitational constant in $\frac{m}{s^2}$.
θ	Is road slope in *radians*.
ρ	Air density $\frac{kg}{m^3}$.

The associate editor coordinating the review of this manuscript and approving it for publication was Miadreza Shafie-Khah.

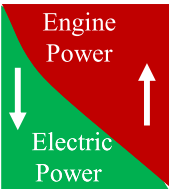|	
A	Frontal area of vehicle in m^2.
C_r	Coefficient of rolling resistance.
C_d	Coefficient of aerodynamic drag.
v	Driving speed in $\frac{m}{s}$.
a	Acceleration of the vehicle in $\frac{m}{s^2}$.
R	Radius of curvature.
N	Normal force perpendicular to the rolling surface in N.
P_i	Tyre pressure in $\frac{N}{m^2}$.
Q_g	Heat generated by battery.

Q_C	Heat generated by chemical reactions in a battery.
Q_J	Joule heat.
Q_{Conv}	Convection of battery heat.
Q_{Cond}	Conduction of battery heat.
ΔH	Change in Enthalpy.
M	Mass of reactants.
n	Reaction order.
A	Pre-exponential factor.
E_a	Activation energy.
R	Gas constant.
T_b	Battery temperature.
T_{air}	Ambient temperature.
I	Current.
U_{OC}	Open circuit voltage.
U_t	Terminal voltage.
h	Convective heat transfer coefficient.
A_s	Battery surface area.
K	Thermal conductivity of battery cover/ surface.
ρ	Density of the battery.
C	Specific heat.
t	Time.
F_{rrf}	Rolling resistance force.
F_{adf}	Aerodynamic drag force.
F_{gdf}	Gradient force.
F_{trf}	Traction force.
$C_{r0}, C_{r1}, C_{r2} \& C_{r3}$	Tyre constants.
$\alpha, \beta, a, b \& c$	Tyre coefficients.
Δz	Rate of change of height in meters per second.
Δm	Inertial factor.
v_f	Final speed of the vehicle in m/s.
v_m	Maximum speed of the vehicle in m/s.
v_g	Gradient speed of the vehicle in m/s.
v_b	Motor speed in m/s.
LIB	Lithium-ion batteries.
EV	Electric vehicle.
BEV	Battery electric vehicle.

I. INTRODUCTION

Carbon-dioxide (CO_2) is one of the primary greenhouse gas (GHG). According to US Environmental Protection Agency (EPA), CO_2 emissions have raised from 14% in 2014 to 27% in 2019 to 30% in 2020. The transportation sector i.e. cars, trucks, ships, trains, and planes primarily consuming diesel & gasoline accounted for about 27% of total greenhouse gas emissions in 2020 (EPA). Ignoring the global economic crisis period of 2007-2008, a regular rise in GHG emissions at an average of 4.7 gigatonnes annually was observed in the last two decades. With a target to decrease GHG emissions, UN Framework Convention on Climate Change agreed to reduce the present CO_2 emissions of the transport sector by 50% by 2050. The possible solution includes the

increased efficiency of vehicles and overall transportation system, deploying low emissions fuels, and promoting the use of zero-emission vehicles i.e. EVs. The efficiency of vehicles and the overall transportation system can account to reduce GHG emissions by up to 46% [1]. Driving style significantly affects fuel consumption [2]. EVs can primarily be zcategorized as hybrid EV (HEV) and Full EV. Hybrid EV can be further zcategorized as micro, mild, and Full HEV. Full HEV can be plug-in HEV type also. Full EV can be battery (BEV) and fuel cell (FCEV) types. A comparison of different vehicle types based on their drive power is presented in Table 1.

TABLE 1. Comparison of different vehicle type based on their drive power.

Vehicle type	ICE Drive	Electric Drive	ICE V/S EV Power
ICE vehicle	Yes	No	100% Engine Power
Micro hybrid vehicle	Yes	No	
Mild hybrid vehicle	Yes	No	
Full hybrid vehicle (non-plug-in type)	Yes	Yes	
Full hybrid vehicle (plug in type)	Yes	Yes	
BEV	No	Yes	100% Electric Power
FCEV	No	Yes	

The degree of hybridization (DOH) is defined as the ratio of electric motor power to the sum of ICE and electric motor power. When ICE power is zero, the DOH becomes 1 i.e. a Full EV. An EV essentially needs to have an Energy Management System (EMS) to control and coordinate the generation, storage, and flow of energy in the drive train. The EMS helps to meet the need for real-time power requirements to drive the EV which requires a PEC to be deployed in the system. The schematic of such a power train for the BEV is shown in Figure 1.

The guidelines for standardization and applications of electrical and control components are issued by SAE and IEC. The vehicle can be charged at home using domestic power supply with rating of 220-440 volts with the help of an on-board charger. This is typically a slow charging scheme. On contrary, the fast charging can be done at a charging station with a high voltage DC power supply. Usually, the EVs are equipped with a Combined Charging System (CCS) of SAE 1772 or IEC 62196-2 type 1. The low current and voltage supply of the onboard charger and the high current and voltage supply of the charging station combines at junction box. The two types of charging type share the neutral terminal. Three wires are connected from the junction box to the battery.

One of the three wires is functional only with an onboard charging scheme and one with a charging station. The third wire remains common. The charging and discharging occur through the same set of wires. The circuit is so designed that
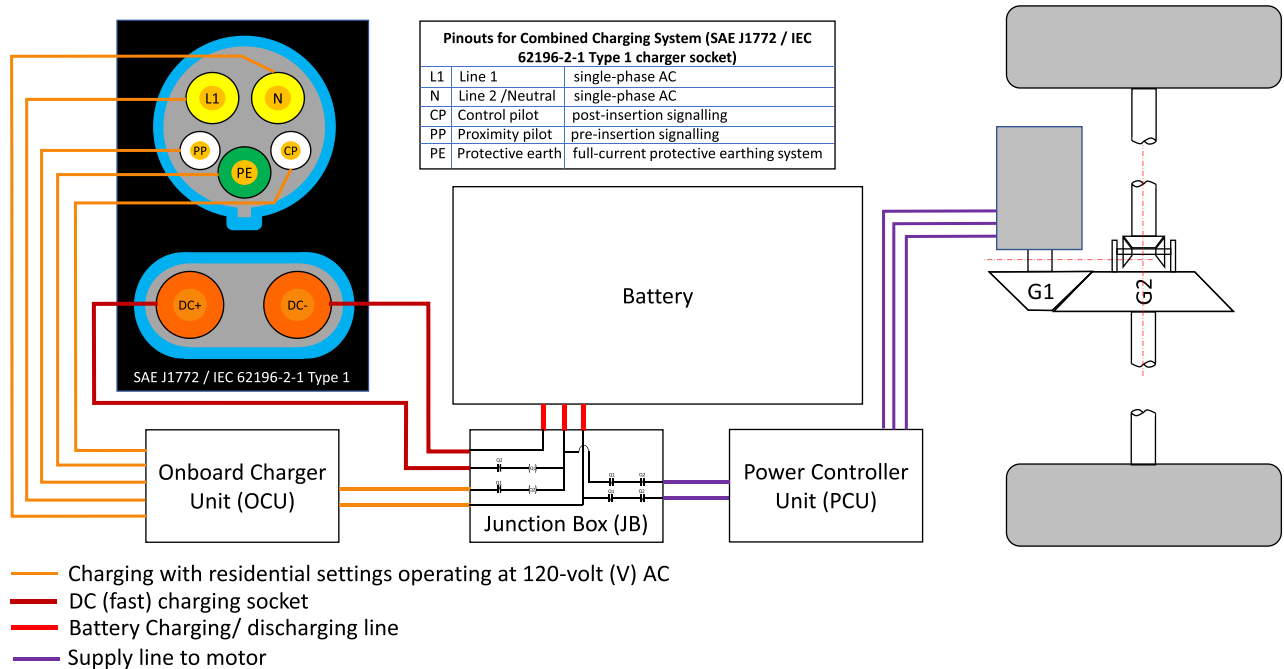
Pinouts for Combined Charging System (SAE J1772 / IEC 62196-2-1 Type 1 charger socket)

L1	Line 1	single-phase AC
N	Line 2 /Neutral	single-phase AC
CP	Control pilot	post-insertion signalling
PP	Proximity pilot	pre-insertion signalling
PE	Protective earth	full-current protective earthing system

FIGURE 1. The schematic of power train for a BEV.

at a time only one of the supplies is functional. Also, the supply to the motor is cut off during charging. The PEC is equipped with a microcontroller to operate the three-phase motor with single-phase DC supply. Along with the power supply, the parallel control and safety buses are also connected to different devices. The data is collected through these buses by the microcontroller unit. The vehicle is usually equipped with a Vehicle Control Unit (VCU) also like Engine Control Unit (ECU). The function of the VCU is analogous to ECU. The auxiliary power supplies are usually controlled through VCU. In addition, the EVs are also equipped with several junction boxes containing fuses, relays, and other functions to ensure the safety and control of the vehicle. There are several different types of risks associated with the use of EVs. These are sometimes life hazardous also. Primarily these can be operational risks and life risks. Talking about the operational risks, the thermal run out of the battery and diffusion of lithium-ion with the electrodes are two severe problems in addition to current leakage. Current leakage can be taken care of in design and manufacturing.

EVs have emerged with a recognition of environment-friendly transportation systems. The efficiency of EVs needs to be studied with varying driving and road conditions. Analysis of experimental observations of EVs is necessarily required to develop energy consumption characteristics for the development of energy-efficient EVs. Driving behavior and driving patterns are then found to be the most significant factors for the analysis of vehicular efficiency and energy consumption. Driving patterns are found to be dependent on distance driven, road topography, and traffic conditions primarily [3]. The gradient of the road greatly impacts vehicle energy consumption. Regenerative braking reduces emissions and increases vehicular efficiency [4].

With difficulty in direct measurement of road gradient, the claim that EVs are less impacted by road gradient as compared to conventional vehicles [5], [6], [7] seems to be impractical. This exists because of a gap in understanding and analyzing the effects of road gradient on energy consumption. Rolling resistance, air drag and gradient [8], intensity of traffic [9], vehicle automation [10], driving style [11], and weather influences [12] are the major influential factors that affect the energy efficiency of EVs.

The auxiliary power requirements are claimed to be constant in many studies as their influence on the performance is less. In a study by Holmberg and Erdemir [13], more than 50% of the total energy supplied by the battery is consumed to overcome the driving resistances, primarily the friction losses and the aerodynamic drag. An energy prediction model should also include driving constraints and limiting conditions, auxiliary power requirements, and their inflations. It is also predicted that the BEV will lead to energy independence in the future [14]. Modelling and analysis are necessary for energy optimization [15]. Cyber-Physical System (CPS) also supports the optimization of algorithms and models [16]. Regenerative braking enhances energy savings in EVs [17]. Regression analysis can be used for energy optimization processes in BEVs [18]. MATLAB & Simulink tools are significant in the modelling and analysis of BEV models [19], [20]. Energy consumption calculations are most desirable in EV [21]. Driving cycles are necessary to examine the performance of EVs [22]. Routing is the highest influential factor for energy consumption [23]. The application

of Artificial Intelligence will optimize the performances of EVs [24]. Variables like routes, environmental factors, traffic, weather, driving styles, and infrastructure, also need to be included in the prediction model. Mathematical models, block diagrams, flow charts, state transition diagrams, bond graphs, etc. are widely used for modeling and simulating energy requirements.

In addition to high energy density with stable performance characteristics and a large number of charging-discharging cycles, the performance of Lithium batteries is badly influenced by extreme conditions of temperature, overcharging, over-discharging, charging, and discharging rates (commonly called C rate). Though the battery operating temperature range is in the range of 10 to 40 degree Celsius, on one hand where it is badly influenced by higher temperatures which might lead to thermal run-away, on the other hand, the chemical reaction and charge transfer rate reduces with a reduction in operating temperature [25], thereby decreasing the conductivity of the electrolyte [26] leading to diffusion of lithium-ion with the electrodes [27]. In countries like Russia, Canada, and Greenland, where the ambient temperature falls below 0 °C, the LIB needs to preheat before usage to avoid its damage [28], [29]. In the case of pure electric vehicles (EVs), hybrid electric vehicles (HEV), and plug-in hybrid electric vehicles (PHEV), it is necessary to preheat the battery before use [30].

Modeling and simulation of EV is necessary to develop vehicle configurations with optimal performance [31]. Different EVs have different configurations, hence need to be modeled and simulated accordingly for their optimal performance. The simulation and validation aim to optimize driving range based on the vehicle type i.e. shape, curb weight, payload, driving style, driving speed, and drive cycle [32]. Equation-based modeling techniques best suited for the dynamic simulation of EVs [31]. Madziel and Campisi in their study on energy consumption by EVs with an existing mathematical model using Python programming felt the need for accurate mathematical models for reliable results [33]. Halabi and Tarabsheh modeled EV dynamics, transmission, and battery using Matlab and verified that the accuracy of the available mathematical models is 73% [34]. This demands the need for the development of new robust mathematical models for EVs. Wei et al. also felt the need for an accurate mathematical model of EVs for the estimation of the driving range [35].

As with static and dynamic vehicle modeling and simulation, thermal management of the LIBs is equally important so that the deployed LIBs could meet the design requirements. This is because, with the increase in the battery temperature, its performance deteriorates drastically, and even reach the condition of thermal runaway beyond some range depending on the battery type. On the other hand, if the battery temperature falls below a certain range, the electrolyte vanishes. Prediction of thermal faults and runaways of LIBs are critical for the durability of EVs [36]. Thermal management is

necessary for the optimal efficiency and life of LIBs [37], [38]. Thermal management usually works with phase change material, air, or liquid [39]. is Easy to use and low cost making liquid and air-cooling more suitable [40].

The electrification of the transportation sector has gained worldwide acceptance as a crucial step towards achieving net-zero emissions and addressing carbon footprints. As a result, there has been a significant increase in research on electric vehicles (EVs) in recent years. Mathematical models have emerged as pivotal tools in advancing the study of EVs. However, one of the major barriers to widespread EV adoption remains the high cost associated with EVs, making it essential to reduce their expenses.

Among the various modeling approaches, the Discrete Choice Model (DCM) has been widely used for EV analysis. Its successor, Agent-Based Modeling (ABM), has also gained attention in the field. While a few researchers have explored the application of machine learning methods in EV modeling, the utilization of revealed preference (RP) datasets to forecast the future of EVs is more common.

Mathematical modeling has been recognized for its valuable contribution to facilitating the transition from ICEVs to EVs. However, the availability of personalized and parameterized data concerning travel behavior specific to EVs is still limited, which poses a challenge for accurate EV simulations. It is crucial to construct mathematical models of EVs carefully, as no model can entirely capture all real-world situations at present. To address this limitation, researchers are actively performing sensitivity analyses to assess the robustness of existing mathematical models in the presence of uncertainties.

In summary, the importance of mathematical modeling in the study of EVs cannot be overstated. While the field has made significant progress, the reduction of EV costs remains a critical factor for achieving large-scale EV adoption globally. Further advancements in modeling techniques, incorporation of personalized data, and rigorous sensitivity analysis will contribute to the development of more accurate and reliable mathematical models for EVs.

In the present study, a novel mathematical model for the prediction of the energy efficiency of an electric vehicle is proposed based on various longitudinal parameters as major driving forces. All other power requirements are considered constant and termed as an auxiliary power of the vehicle. This research article reviews the various existing models of vehicular energy calculations under different driving conditions and proposes a new mathematical model with wider perspectives and depth in its scope. The performance of the proposed novel mathematical model is studied for different driving conditions. The accuracy of the proposed model is also tested for different driving cycles. The performance of the proposed model is also compared with existing models with varying rolling resistance force, aerodynamic drag, and gradient force under different test conditions. The effect of temperature variation on the performance of the vehicle is

then studied at the end of the research article. A suitable Pneumatic-Liquid Thermal Management System (PLTMS) is also discussed. The proposed model is developed to work under the dynamic parameters of an EV like, Tyre pressure, Vehicular velocity, Dynamic rolling resistance coefficient, and Direction of vehicle travel concerning wind velocity.

The article provides a systematic approach to understand and optimize the driving forces that influence EV performance and sustainability. In our study, we have modelled rolling resistance, aerodynamic drag and gradient forces from a different perspective. The mathematical formulations of the EV for torque and power calculations in this research article will make a significant contribution in the field of electric vehicles. This model can be used to analyze and predict EV behavior under different driving conditions, road types, and terrains, allowing for the design and implementation of more efficient and sustainable EV systems. The contribution of this research is crucial in the pursuit of sustainable EV operation as it aids in the development of advanced energy management strategies, optimized powertrain designs, and the identification of potential areas for efficiency improvements. Ultimately, this mathematical modeling approach plays a key role in enhancing the overall performance and environmental sustainability of Electric Vehicles, bringing us closer to a greener and more sustainable transportation future.

This current section discussed the introduction and literature review. Section two will focus on the development of an energy prediction model for an EV. The traction model is proposed in section three, followed by results and discussion, and a conclusion in sections four and five respectively.

II. ENERGY PREDICTION MODEL FOR AN EV
To accurately predict vehicular energy consumption, it is necessary to study vehicular dynamics. The different vehicular dynamic parameters of an EV are classified as longitudinal, lateral, and vertical dynamic type. It is extremely important to understand the impact of different driving resistances on the performance of an EV [13]. In this article, the effect of driving resistance on the performance of the vehicle, which is a part of the lateral dynamic parameter, is studied and analyzed. Figure 2 (a) and (b) depict the longitudinal motion & resistances of the vehicle on flat terrain and on an inclined road respectively. The driving force (at the drive axle) is the sum of the moving force of the vehicle and the resistances acting against its motion. The aerodynamic drag and rolling resistances are the two primary resistances acting against the vehicle motion. Aerodynamic drag is a function of air density, frontal area, drag coefficient, velocity of the vehicle, and wind velocity. Rolling resistance, is dependent on the mass of the vehicle, the velocity of the vehicle, and the tyre pressure. The traction power varies with road type (coefficient of rolling resistance changes with change in road type), driving style (type of acceleration), aerodynamic drag, and gradient of the road. The auxiliary power includes power steering, lights, music, air-conditioning, suspension type, tyre slip, and other assistances installed/ equipped in the vehicles.

Primarily the energy consumption model is developed by considering traction forces, auxiliary power requirements, power train efficiency, auxiliary power efficiency, and braking requirements.

A. ROLLING RESISTANCE
The force resisting the vehicle movement is termed rolling resistance. It is usually denoted as the coefficient times of the normal force acting on the vehicle. For a vehicle to just start rolling, it must overcome the rolling resistance. The following models are available in the literature. The result of the proposed model is compared with these existing models.

Model-A.1: According to minimum Heywood [41], rolling resistance can be modeled as:

$$F_{rrf} = C_r mgv \qquad (1)$$

C_r, m, g and v are coefficient of rolling resistance, mass of the vehicle, gravitational force and vehicle velocity respectively. The author assumed the rolling resistance to be directly proportional to the velocity, which gives a linear curve, the possibility of which is contradictory to the theoretical claims in the available literature.

Model-A.2: According to Das and Sharma, [42] the rolling friction force can be modeled as:

$$F_{rrf} = C_r N \qquad (2a)$$

The rolling resistance coefficient (C_r) is a cubic function of the velocity of the vehicle and coefficients of tyre construction, C_{r0}, C_{r1}, C_{r2} and C_{r3} [43] as shown below:

$$C_r = C_{r0} + vC_{r1} + v^2 C_{r2} + v^3 C_{r3} \qquad (2b)$$

C_{r0}, C_{r1}, C_{r2} and C_{r3} are constants having different values. Values of these constants are dependent on tyre type. N is normal force. The value of these constants for a radial tyre is shown in Table 2.

TABLE 2. Value of different coefficients for a radial tyre.

Name of constant	Value of the constant
C_{r0}	1×10^{-2}
C_{r1}	5×10^{-7}
C_{r2}	2×10^{-7}
C_{r3}	1×10^{-7}

Model-A.3: According to SAE-J2452 [44], rolling resistance is dependent on vehicle speed (v) in $\frac{m}{s}$, tyre pressure (P_i) in $\frac{N}{m^2}$ and load (mg), as:

$$F_{rrf} = (mg)^\alpha P_i^\beta \left(a + bv + cv^2 \right) \qquad (3)$$

Table 3 presents values of tyre-dependent coefficients (i.e. α, β, a, b & c) used in eq. (3).

Model-A.4: SAE also recommends using the model proposed by Genta and Morello [45] for rolling resistance, which
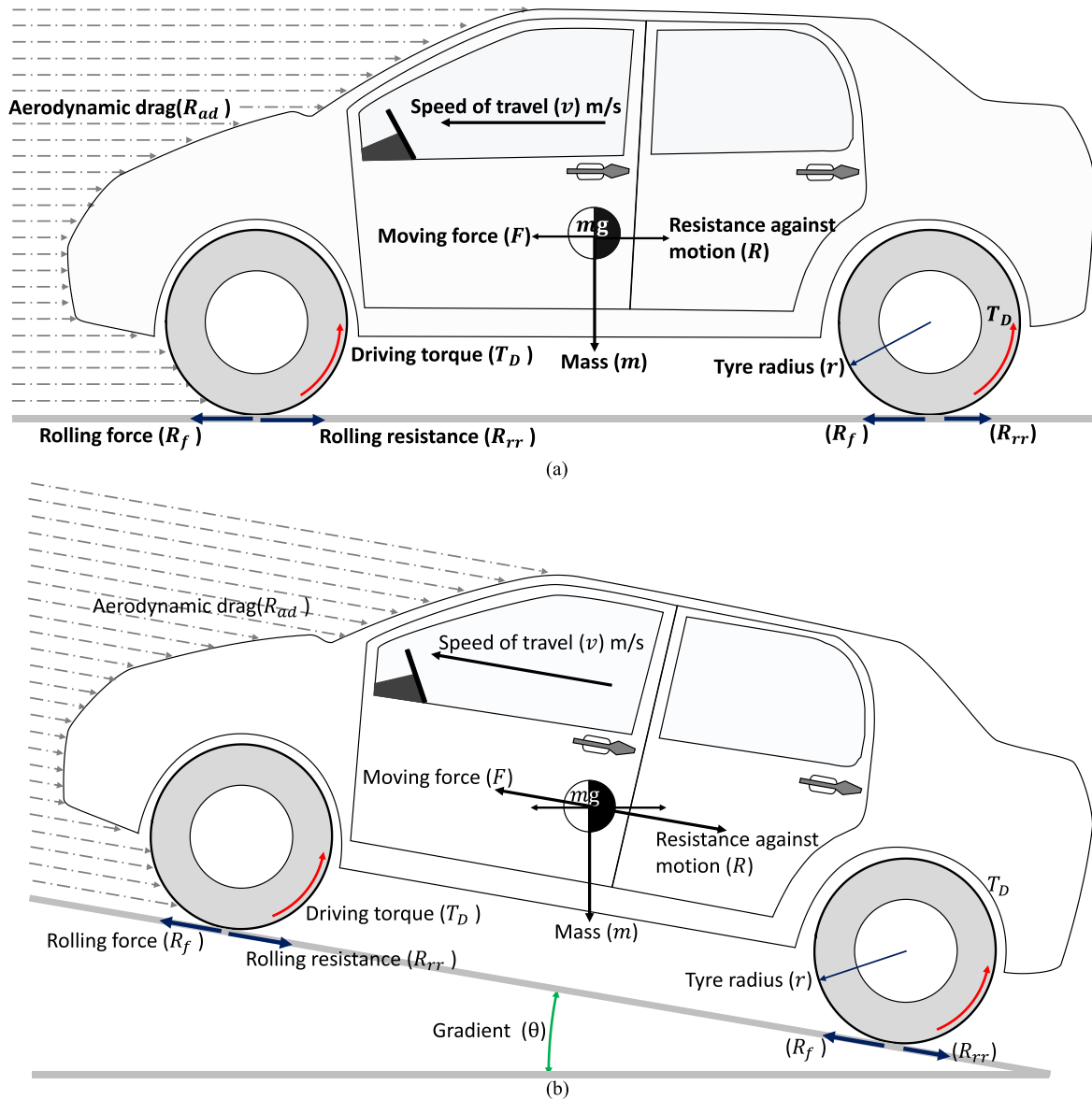
FIGURE 2. (a) Longitudinal motion & resistances of the vehicle on flat terrain. (b). Longitudinal motion & resistances of the vehicle on inclined road (θ is gradient under consideration).

is dependent on tyre pressure (P_i) in $\frac{N}{m^2}$, vehicle velocity (v) in $\frac{m}{s}$, and load (mg) in N as:

$$
\begin{aligned}
\mathrm{F_{rrf}} \\
= \frac{\mathrm{K}}{10^3} \bigg(5.1 \\
+ \frac{\left(5.5 \times 10^5 + 90mg\right) + \left(1.1 \times 10^3 + 3.88 \times 10^{-2} mg\right) v^2}{\mathrm{P_i}} \bigg)
\end{aligned}
\tag{4a}
$$

The constant K is defined as below:

$$
K = \begin{cases} 0.8 & \text{for radial tyres} \\ 1 & \text{for non-radial tyres} \end{cases}
\tag{4b}
$$

During the comprehensive literature review, a recurring theme emerged among researchers studying the modeling and

TABLE 3. Value of tyre dependent coefficients.

Name of coefficient	Value of the coefficient
α	1.03399904
β	$-4.1081927 \times 10^{-1}$
a	5.933157×10^{-2}
b	9.85526×10^{-5}
c	3.72314×10^{-7}

simulations of EVs; the pressing need for a highly accurate and dependable mathematical model to attain optimal EV performance. Given that the cost of BEVs is primarily determined by the costs of LIBs and their associated controls, an in-depth mathematical analysis holds immense potential in optimizing battery power utilization. In light of these considerations, the authors propose a novel mathematical model

that promises enhanced realism and accuracy compared to existing approaches.

Model-A.5: PROPOSED ROLLING RESISTANCE MODEL: To establish a more realistic mathematical model for EVs, it is essential to incorporate the following factors:

1) THE IMPACT OF TYRE PRESSURE ON ROLLING RESISTANCE

Tyre pressure plays a significant role in determining the resistance experienced by the vehicle while in motion. By accounting for the influence of tyre pressure in the mathematical model, a more accurate representation of rolling resistance can be achieved. This consideration acknowledges the direct relationship between tyre pressure and the energy required for vehicle propulsion.

2) THE EFFECT OF VEHICLE VELOCITY ON ROLLING RESISTANCE

It is well-established that rolling resistance varies with the speed at which the vehicle is traveling. By incorporating the influence of vehicle velocity in the mathematical model, a more comprehensive understanding of rolling resistance can be attained. This enables a more nuanced analysis of how varying speeds affect the overall performance and energy efficiency of EVs.

By integrating these factors into the proposed mathematical model, researchers aim to enhance its realism and accuracy, enabling a more precise prediction of rolling resistance in EVs. Considering the above-mentioned effects, the proposed model for rolling resistance, F_{rrf} by the authors is:

$$F_{rrf} = C_r mg \qquad (5)$$

The coefficient of rolling resistance (C_r) is found to be dependent on the ratio of the horizontal pushing force required to roll a tyre in the direction of travel to the vertical load on the tyre. The authors propose to calculate the coefficient of rolling resistance through the following formulation:

$$C_r = \left(\frac{1}{P_i}\right)\left(0.1 + \left(\frac{v}{10^2}\right)^2\right) \qquad (6)$$

The rolling resistance experienced under the given conditions exhibits a range of values from 2.86×10^{-3} to 6.16×10^{-3}. It should be noted that the coefficient of rolling resistance can vary depending on factors such as the type of road surface, pavement type, and tyre pressure. For instance, on asphalt, the coefficient of rolling resistance can be as low as 6×10^{-3}, while on the sand, it can reach as high as 0.4.

To compare the rolling resistance of the five models considered, Figure 3 presents the results under specific virtual test conditions. These conditions include a vehicle load of 1350 kg, a zero gradient $(\theta = 0°)$, the same road surface and pavement type, a constant tyre pressure of 35 PSI, and a vehicle velocity ranging from 0 to 120 kmph.

The literature, comprising various theoretical and experimental studies, has consistently concluded that the variation

in rolling resistance is not significant with changes in vehicle velocity. The proposed model aligns with these findings, as depicted in Figure 3. The rolling resistance values obtained from the model demonstrate a gradual increase as the vehicle speed increases. Specifically, the rolling resistance varies from 61.66 N at the start to 69.15 N at 40 kmph, 73.3 N at 50 kmph, 79 N at 60 kmph, 85.9 N at 70 kmph, 91.6 N at 80 kmph, 100.2 N at 90 kmph, 110 N at 100 kmph, 119.9 N at 110 kmph, and 132.9 N at 120 kmph.

The variation in rolling resistance shows a nearly linear trend within each 10 kmph speed range. Additionally, it is important to note that rolling resistance is dependent on both tyre pressure and vehicle velocity. Tyre pressure, in particular, has a significant influence on rolling resistance.
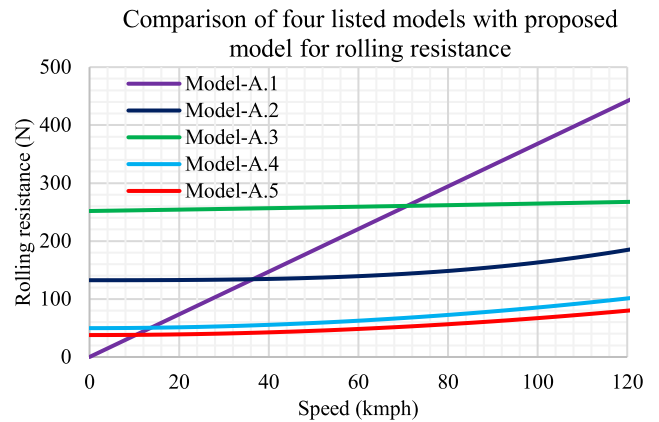

FIGURE 3. Comparison of rolling resistance with the proposed model for different models at 35 PSI pressure.
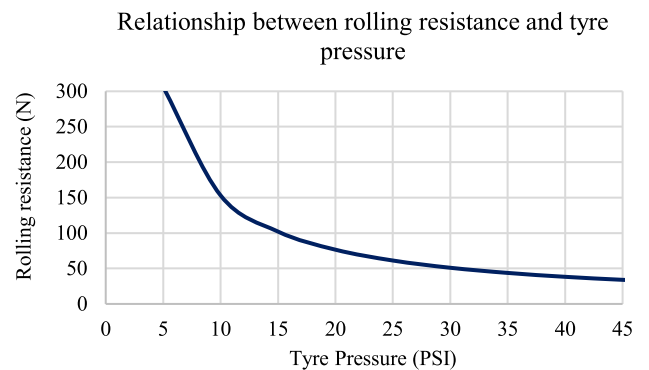

FIGURE 4. Relationship between rolling resistance and tyre pressure.

Figure 4 illustrates the relationship between rolling resistance and tyre pressure, revealing the non-linear nature of this connection. It can be inferred from the graph that as tyre pressure increases further, the variation in rolling resistance becomes minimal, potentially negligible. Consequently, it can be concluded that maintaining appropriate tyre pressure is crucial for ensuring optimal performance in an EV.

To address this, there is a need to incorporate a tyre pressure display on the dashboard panel of EVs. Such a display would not only provide real-time information about

the current tyre pressure but also indicate the optimal range for achieving peak performance. Additionally, the display should present the variations in performance associated with different tyre pressure levels, emphasizing the importance of maintaining the ideal pressure for efficient operation.

B. AERODYNAMIC DRAG FORCES

When the vehicle moves, its movement is opposed by the airflow. The amount of this opposing force, termed aerodynamic drag force depends on the frontal area of the vehicle, the coefficient of aerodynamic drag, and the vehicle velocity.

Model-B.1: The aerodynamic drag force proposed by Heywood [41], Cauwer et. al [46], and Berry [47] is given as:

$$F_{adf} = \frac{1}{2}\rho A C_d v^2 \qquad (7)$$

Model-B.2: Ehsani et al. [48] recommended the following model for the maximum speed of the vehicle:

$$F_{adf} = \frac{1}{5}\rho A C_d v^2 \qquad (8)$$

The analysis of the aforementioned models highlights an important aspect that has been neglected, i.e. the impact of gradient slope on aerodynamic drag. To ensure accurate estimations of battery capabilities, it is crucial to comprehend the performance of EV in hilly terrains as well.

Model-B.3: PROPOSED AERODYNAMIC DRAG MODEL: In light of this, the authors propose an enhanced Aerodynamic Drag Model that considers the influence of gradient in aerodynamic force calculations. It is well-established that aerodynamic drag forces have an exponential relationship with vehicular speed. By incorporating the effect of the gradient in these calculations, the proposed mathematical model becomes more realistic and comprehensive. The model can provide valuable insights into performance and energy consumption under diverse scenarios. This knowledge is vital for optimizing battery usage and ensuring the efficient operation of EVs in real-world conditions. The authors propose following aerodynamic drag model (F_{adf}):

$$F_{adf} = \frac{1}{2}\rho A C_d \left(v\left(1 + \sin\theta\right)\right)^2 \qquad (9)$$

Air density ρ at NTP is 1.2 $\frac{kg}{m^3}$, which varies with changes in meteorological data, because of which the actual drag forces vary in experimentation in different terrains. The frontal area A remains constant for a vehicle type under study and experimentation. The value of the drag coefficient depends on frontal area, body shape, Reynolds Number, Froude number, Mach Number, and surface finish ranging from 0.2 to 0.9 [49]. The change in terrain can be accommodated by conducting simulations with varying air density in addition to variation in other variables of the above model.

Under the same test conditions, the comparison of the aerodynamic drag for the above three models for an EV with 1.6 m width and 1.5 m height, 0.3 as drag/ wind speed coefficient and 1.2 $\frac{Kg}{m^3}$ as the density of air (at NTP) is presented in Figure 5.
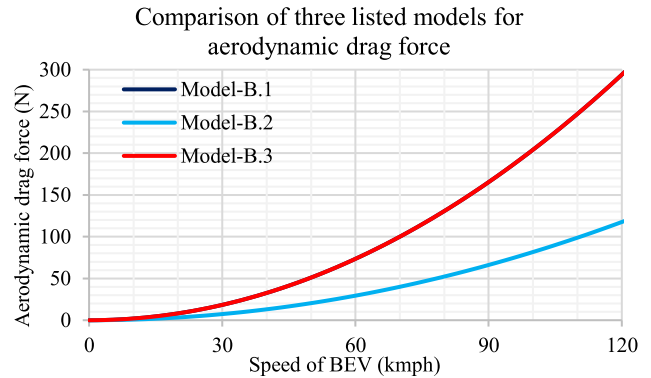

Comparison of three listed models for aerodynamic drag force

FIGURE 5. Comparison of the aerodynamic drag for different models.

Analyzing the aforementioned considerations, the authors put forth a novel and improved Aerodynamic Drag Model that takes into consideration the influence of gradient in aerodynamic force calculations. Extensive research has established that aerodynamic drag forces exhibit an exponential relationship with vehicular speed. However, the influence of gradient on aerodynamic forces has often been overlooked. Table 4 represents the variation in aerodynamic drag force w.r.t. the change in gradient. From the table, it can be inferred that the change in aerodynamic drag force is approximately 0.06% and 0.03% per degree change in the gradient at 60 kmph and 120 kmph respectively.

TABLE 4. Percentage variation in aerodynamic drag force (KW) w.r.t. variation in gradient.

Gradient	Vehicle Speed				
	40 kmph	60 kmph	80 kmph	100 kmph	120 kmph
1°	0.087	0.058	0.044	0.035	0.029
2°	0.175	0.116	0.087	0.070	0.058
3°	0.262	0.175	0.131	0.105	0.087
4°	0.349	0.233	0.174	0.140	0.116
5°	0.436	0.291	0.218	0.174	0.145
6°	0.523	0.349	0.261	0.209	0.174
7°	0.610	0.407	0.305	0.244	0.203
8°	0.697	0.464	0.348	0.279	0.232
9°	0.784	0.522	0.391	0.313	0.261
10°	0.870	0.580	0.435	0.348	0.290

By incorporating the effect of gradient into the aerodynamic force calculations, the proposed mathematical model gains heightened realism and comprehensiveness. This enhancement allows for a more accurate representation of the complex dynamics involved in EV performance. The model becomes capable of providing valuable insights into the intricate interplay between aerodynamic drag, gradient, vehicle speed, and their impact on energy consumption and overall performance under diverse driving scenarios.

The proposed aerodynamic drag model plays a pivotal role in optimizing battery usage and ensuring the efficient operation of EVs in real-world conditions. By accurately capturing the influence of gradient on aerodynamic forces, the model empowers researchers, engineers, and EV manufacturers to fine-tune their designs, develop effective control strategies,

and make informed decisions regarding battery capacity and energy management systems.

With its ability to provide a comprehensive understanding of the performance and energy consumption of EVs under various scenarios, this proposed model is a valuable tool for the development and advancement of sustainable transportation. It holds immense significance in optimizing EV efficiency, extending driving range, and promoting the widespread adoption of electric vehicles as a viable alternative to traditional combustion-engine vehicles.

C. GRADIENT FORCES

There are highs and lows on the road. These highs and lows develop gradients on the road. These highs need additional forces to climb up. The generalized formulation for the calculation of the gradient force F_{gdf} is given by:

$$F_{gdf} = mg \sin \theta \tag{10}$$

The existing mathematical model of the gradient force fails to incorporate the variations in tyre pressure and the vehicle velocity.

Model-C.1: PROPOSED GRADIENT FORCES MODEL: The current mathematical model of the gradient force neglects crucial factors such as variations in tyre pressure and vehicle velocity, limiting its realism and accuracy. To address these limitations and create a more comprehensive and robust model, the authors propose the following enhancements:

1. ***Influence of tyre pressure during travel on a gradient:*** The proposed model recognizes the significant influence of tyre pressure on the gradient force experienced by the vehicle. By incorporating the effect of tyre pressure variations in the mathematical calculations, the model becomes more realistic, accounting for the changes in force resulting from different tyre pressures.
2. ***Influence of velocity during travel on a gradient:*** The proposed model also considers the impact of vehicle velocity on the gradient force. It acknowledges that the force exerted by the gradient varies with the speed at which the vehicle is traveling. By incorporating the influence of velocity in the mathematical calculations, the model becomes more accurate, capturing the dynamic nature of the gradient force in different driving conditions.

By integrating these factors into the proposed mathematical model, the authors aim to enhance its realism, accuracy, and robustness. The resulting model provides a more comprehensive understanding of the gradient forces acting on the vehicle, accounting for the effects of tyre pressure and velocity. This advancement is crucial for accurately estimating the forces encountered during travel, enabling more precise predictions of vehicle performance, optimizing battery usage, and ensuring efficient operation of Electric Vehicles (EVs) in real-world conditions. The authors proposed the following novel mathematical model of the gradient force:

$$F_{gdf} = F_{rrf} \sin \theta = (C_r mg) \sin \theta \tag{11a}$$

where,

$$C_r = \left(\frac{1}{P_i}\right)\left(0.1 + \left(\frac{v}{100}\right)^2\right) \tag{11b}$$

The calculations of the coefficient of rolling resistance (C_r) are to be calculated as done in section II-A.

In this study, the authors introduce three distinct models to address different aspects of Electric Vehicle (EV) design. These models include the novel Rolling Resistance Model (Section II-A), Aerodynamic Drag Model (Section II-B), and Gradient Model (Section II-C). Each of these models brings forth unique insights into the forces and factors influencing EV performance.

To establish a comprehensive approach to EV design calculations, it is essential to integrate these three proposed models into a unified traction model. The integrated traction model provides a holistic understanding of the forces that impact EV performance. This integrated model will enable researchers, engineers, and designers to conduct more accurate and comprehensive calculations for various aspects of EV design to optimize EV design parameters, evaluate energy efficiency, and make informed decisions regarding battery capacity, powertrain systems, and overall vehicle performance.

III. PROPOSED TRACTION MODEL

According to minimum Heywood [41], power (E_{He}) required to start a vehicle to move is the sum of the power required to overcome aerodynamic drag and rolling resistance, the same can be mathematically written as:

$$E_{He} = \left(\frac{1}{2}\rho A C_d v^3\right) + (C_r mgv) \tag{12}$$

This power model i.e. energy required to move a vehicle lacks the gradient forces in it, also the rolling resistance is assumed to be directly proportional to the velocity, which gives a linear curve, the possibility of which is rare. Thus, this model fails to predict the actual energy requirements for a vehicle. Cauwer et. al [46] and Berry [47] updated the model by incorporating the force required to accelerate the vehicle and the gradient force to climb a slope. The energy consumption model given by [46] is:

$$E_{Ca} = (mva) + \left(\frac{1}{2}\rho A C_d v^3\right) + (mg\Delta z) + (C_r mgv) \tag{13}$$

where Δz is the rate of change of height in meters per second. Again, in this model rolling resistance is assumed to be directly proportional to the velocity, with similar constraints as given by Heywood. Thus, this model again fails to predict the actual energy requirements for a vehicle. The energy consumption model given by Berry is [47]:

$$[E_{Be} = (mva) + \left(\frac{1}{2}\rho A C_d v^3\right) + (mvg \sin \theta) + (C_r mvg \sin \theta)] \tag{14}$$

Again, in this model rolling resistance is assumed to be directly proportional to the velocity. They also introduced

$cos\, cos\, \theta$ term with the rolling resistance force, which reduces the rolling resistance when moving on a gradient, which again turns doubtful. Combining *mvg sin sin θ* and C_r*mvg cos cos θ* again gives the same results as given by Cauwer et al. [46]. Thus, this model again fails to predict the actual energy requirements for a vehicle. Ehsani et al. [48] proposed the following three different models for acceleration, maximum speed & grading:

$$P_{acc} = \left(\frac{\Delta m}{2t} \left(v_f^2 + v_b^2 \right) \right) + \left(\frac{2}{3} C_r mg v_f \right) + \left(\frac{1}{5} \rho A C_d v_f^3 \right) \tag{15}$$

where Δm is the inertial factor, t is acceleration time, v_f, v_m, v_g and v_b are the final, maximum, and gradient speed of the vehicle and motor speed respectively in m/s. this model has again similar problems in considering rolling resistance as a function of velocity.

The forces required to travel are called traction forces. According to basic physics, the traction force (F_{trf}) of an automobile vehicle is dependent on rolling resistance (F_{rrf}), aerodynamic drag forces (F_{adf}) and gradient forces (F_{gdf}). Thus, the traction force (F_{trf}) requirements of an automobile vehicle can be modeled as:

$$F_{trf} = F_{rrf} + F_{adf} + F_{gdf} \tag{16}$$

The traction forces are independent of the fuel type. i.e. are same for ICEVs and EVs. Figure 6 presents drive cycle data used in this study to estimate the power demand in real-time drive. The power demand for the drive cycle under consideration is shown in Figure 7.

The proposed model, known as the Realistic Mathematical Traction Model (RMTM), offers several advantages over existing models found in the literature and is recommended by SAE for Original Equipment Manufacturers (OEMs) and car manufacturers. The RMTM incorporates the following key features:

1. **Tyre pressure in rolling resistance formulation:** Unlike existing models, the RMTM includes a more realistic empirical formulation that considers the influence of tyre pressure on rolling resistance. By incorporating this crucial factor, the model provides a more accurate representation of the forces encountered during vehicle operation.
2. **Vehicle velocity in rolling resistance formulation:** The RMTM also incorporates vehicle velocity as a significant factor in rolling resistance formulation, employing a realistic empirical formulation to capture the influence of speed on resistance. This ensures a more precise estimation of rolling resistance under varying driving conditions.
3. **The gradient in aerodynamic drag force calculations:** The RMTM takes into account the influence of gradient on aerodynamic drag forces. This feature is absent in many existing models and is an important factor in accurately predicting the forces experienced by the vehicle in hilly terrains or sloping roads.
4. **Consideration of rolling resistance and its dependence on tyre pressure and vehicular velocity in gradient force**

calculations: The RMTM uniquely incorporates the influence of rolling resistance, which is further dependent on both tyre pressure and vehicular velocity, in gradient force calculations. This aspect has not been reported in any previously published research articles, making the RMTM more comprehensive and realistic in its approach.

By encompassing these advancements, the proposed traction model offers numerous benefits for EV design calculations. It provides a more accurate estimation of power requirements and energy consumption during various driving conditions. Furthermore, the model's power calculations are analyzed using a drive cycle depicted in Figure 6, and the vehicular specifications and model parameters are detailed in Table 5, ensuring a comprehensive evaluation of EV performance.

TABLE 5. Model parameters for vehicular specification considered under analysis.

Model Parameter	Values
Curb weight	1350 kg
Motor power	25 kW
Peak torque	320 N-m
Final drive ratio	17:64
Battery capacity	60 kWh
Initial Acceleration	(0–60 kmph) in 7.5 s
Aerodynamic drag coefficient	0.175
Tyre specifications	165/65 R14 79T
Radius of tyre	292 mm
Efficiency of gear system	95%

With the above model parameters, the Model design parameters values are presented in Table 6. These values are vetted in comparison with several standard design values from several different sources.

TABLE 6. Model design parameters values.

Parameter	Description	Value
ρ	Air Density (at NTP)	1.23
C_d	Aerodynamic drag coefficient	0.38
P_i	Tyre pressure	25-45 PSI
A	Vehicle Frontal Area	2.5
v	Vehicle Speed	0 to 60 kmph
a	Vehicle acceleration	0–60 mph
m	Vehicle mass	1350
g	Gravity	9.81
θ	Degrees Road angle	0 - 10°

Based on the given parameter values and utilizing the drive cycle data depicted in Figure 6, the power demand for the EV is calculated, and the results are presented in Figure 7. It is observed that the power demand curve exhibits a similar pattern to the drive cycle data, indicating that the proposed model successfully captures the dynamics of power requirements during vehicle operation. This alignment between the calculated power demand and the actual drive cycle data validates the accuracy and reliability of the proposed model.

Furthermore, the state of charge (SOC) curve of the battery, derived from the proposed model, is illustrated in Figure 8. The SOC curve provides insights into the battery's energy
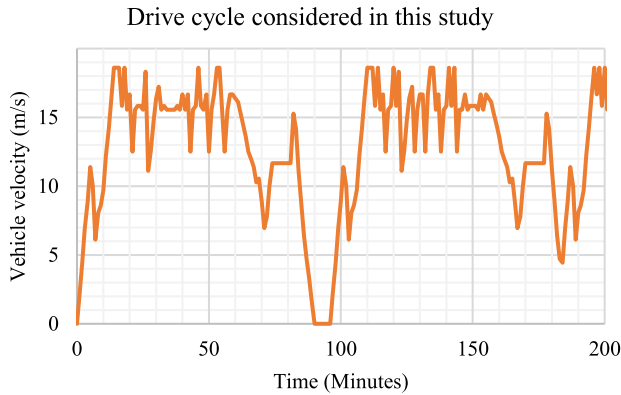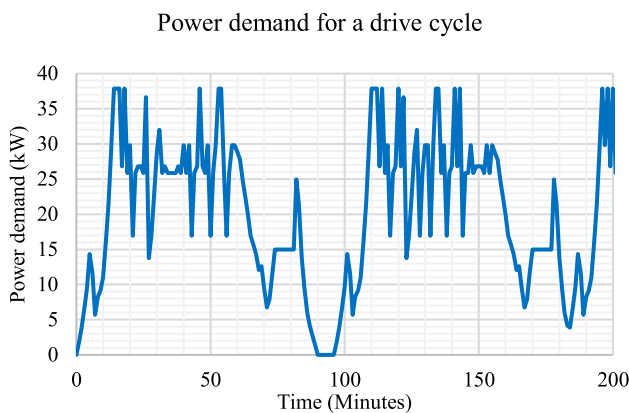
Drive cycle considered in this study

FIGURE 6. Drive cycle considered in this study.

Power demand for a drive cycle

FIGURE 7. Power demand for the drive cycle under consideration.

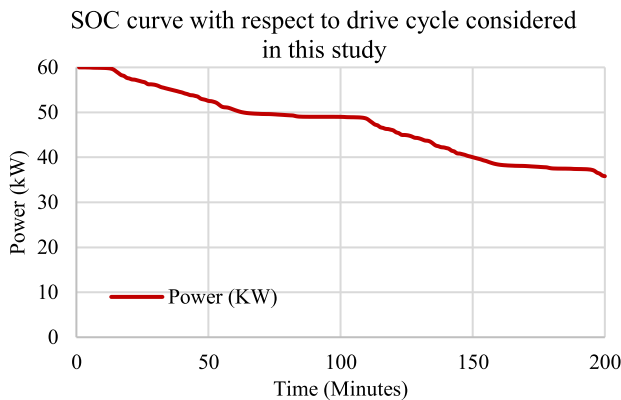SOC curve with respect to drive cycle considered in this study

FIGURE 8. State of Charge curve of the lithium-ion battery.

storage and depletion throughout the drive cycle. By considering various factors such as rolling resistance, aerodynamic drag, and gradient forces, the proposed model accurately estimates the SOC of the battery, allowing for a more comprehensive evaluation of the EV's energy management.

Analyzing the drive cycle data, it is determined that the average speed of the vehicle is 5.9 m/s. Using this average speed and a drive cycle duration of 200 minutes, it can be projected that the vehicle will cover a distance of approximately 64 km. This estimation accounts for the vehicle's

performance and energy consumption characteristics as represented by the proposed model.

The model's ability to accurately estimate power demand and battery SOC contributes to the development of more efficient and reliable EV systems, supporting the widespread adoption of sustainable transportation solutions.

The RMTM represents a significant step forward in the field of EV design and analysis, offering improved accuracy, realism, and a comprehensive understanding of the complex factors influencing EV traction and power requirements. Its advancements enable engineers and researchers to make more informed decisions regarding EV design, optimizing performance, efficiency, and overall user experience.

IV. EFFECT OF TEMPERATURE ON EV

It is worthwhile to note that the operating temperature of the vehicle is also a critical factor and plays a vital role in specifying the sustainable operation of the electric vehicle [49], [50], [51]. A temperature change significantly impacts the charge/discharge capacity of the lithium-ion batteries and eventually the performance of the electric vehicle [52]. The performance of the lithium-ion batteries (LIB) degrades significantly. the temperature alone can lead to a reduction of about 50% in the vehicle range as discussed in [53] and [54].

The variation in the life cycle of a LIB at different operating temperatures for 1C rate is simulated and presented in Figure 9. It is visible from the graph that the battery pack has maximum life when operated near 25 °C. It is worth noting that the life cycle changes drastically in the regions where the operating temperature range is wide. The life cycle is affected by almost 4%, 6%, 7.8%, 10%, 12%, and up to 23.5% with the temperature variation of 30 °C, 36 °C, 42 °C, 47 °C, 51 °,C and 71 °C respectively. This justifies the need to develop a suitable Thermal Management System (TMS). This would help to regulate and maintain the temperature of its components. The system generally uses a combination of heating and cooling mechanisms, such as liquid coolant circuits, air cooling, and insulation, to keep the components within their optimal operating temperature range. This is important for improving the performance and longevity of the components and ensuring the safe and reliable operation of the EV.

A literature survey on TEC-based BTMS was conducted by Siddique et al. [55]. The study covered a period of 2003-2018 and showed that there has been an increase in the use of TEC-based BTMS over time. In another study from [56], the various modeling methods of thermoelectric elements and thermoelectric coolers were discussed. In [57], the researchers proposed a thermal management system based on thermoelectric cooling, forced air cooling, and liquid cooling. This experimental study examined the battery thermal behaviour at different voltage levels, typically in the range from 30V to 60V under natural cooling and hybrid thermoelectric cooling methods. Li et al. [58] presented a similar temperature-controlled system using direct cooling.
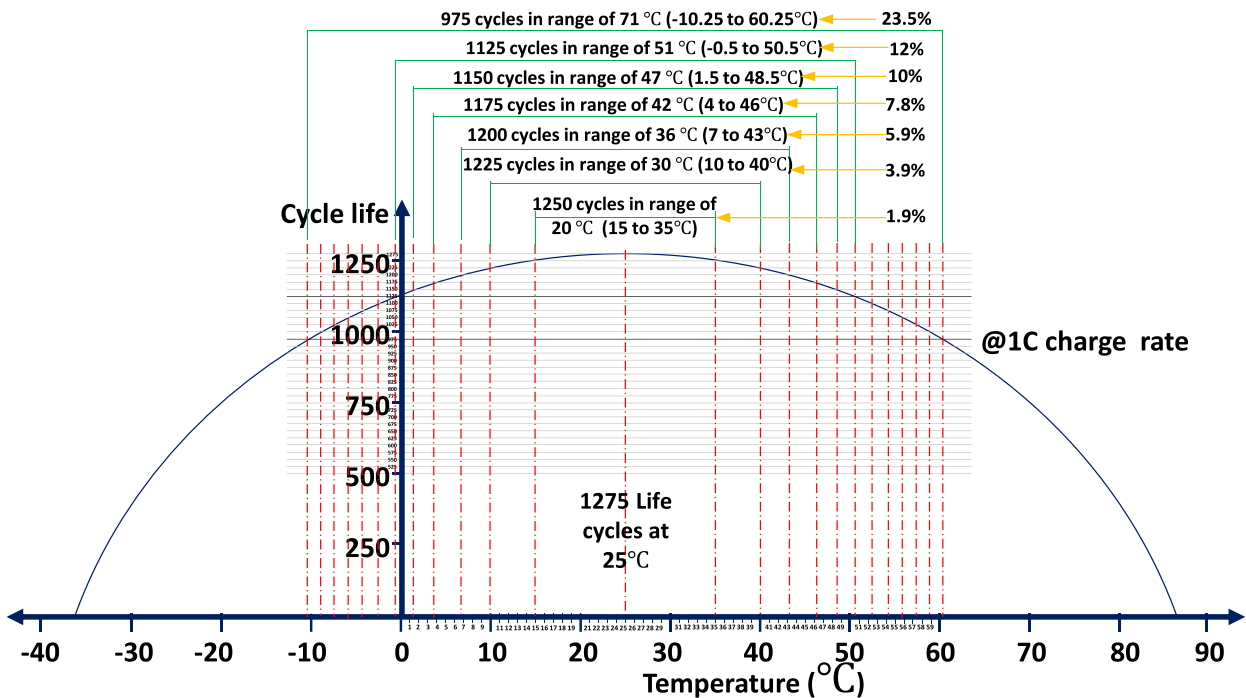
FIGURE 9. Variation in LIB life cycles for different temperature ranges.
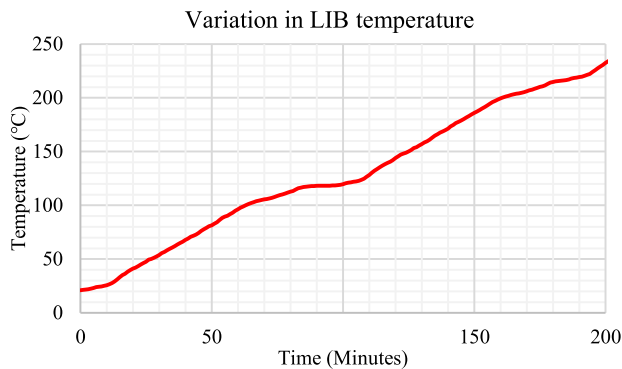

FIGURE 10. Change in temperature of the battery without any active thermal management system.

This BTMS used an electronic coolant that was circulated through the airducts and then piped directly into the device during power up without using any other coolant or media. Qin et al. [59] proposed the use of forced-air convection for battery thermal management system.

A. THERMAL MODELING OF LITHIUM-ION BATTERIES (LIB)

To understand the thermal properties of LIB and EV as a whole, it is important to model the thermal impact mathematically. The heat generated by a battery is the combination of heat generated during the chemical reaction and Joule heat as given by Liu et al. [60]:

$$Q_g = Q_C + Q_J \tag{17}$$

$$Q_g = \Delta HM_n A exp\left(-\frac{E_a}{RT_b}\right) + I\left(U_{OC} - U_t\right) \tag{18}$$

General formulation of convection of battery heat to air from the battery can be expressed as:

$$Q_{Conv} = hA\left(T_b - T_{air}\right) \tag{19}$$

Heat conduction between the battery surface and ambient air can be expressed by:

$$Q_{Cond} = KA\left(T_b - T_{air}\right) \tag{20}$$

Considering uniform temperature distribution across the battery, the variation in the temperature of the battery with cover is expressed as:

$$C\frac{\partial T_b}{\partial t} = \Delta HM_n A exp\left(-\frac{E_a}{RT_b}\right) + I\left(U_{OC} - U_t\right) - KA\left(T_b - T_{air}\right) \tag{21}$$

And the variation in the temperature of the battery without cover is expressed as:

$$\frac{\partial T_b}{\partial t} = \Delta HM_n A exp\left(-\frac{E_a}{RT_b}\right) + I\left(U_{OC} - U_t\right) - hA\left(T_b - T_{air}\right) \tag{22}$$

Research is still finding solutions to enable Lithium batteries to operate at higher temperatures with optimum performance. Liquid and air cooling and the use of phase change materials are the three applicable cooling techniques. Individual as well as hybrid cooling techniques are in practice. Hybrid (cooling schemes combining liquid, air, and phase change
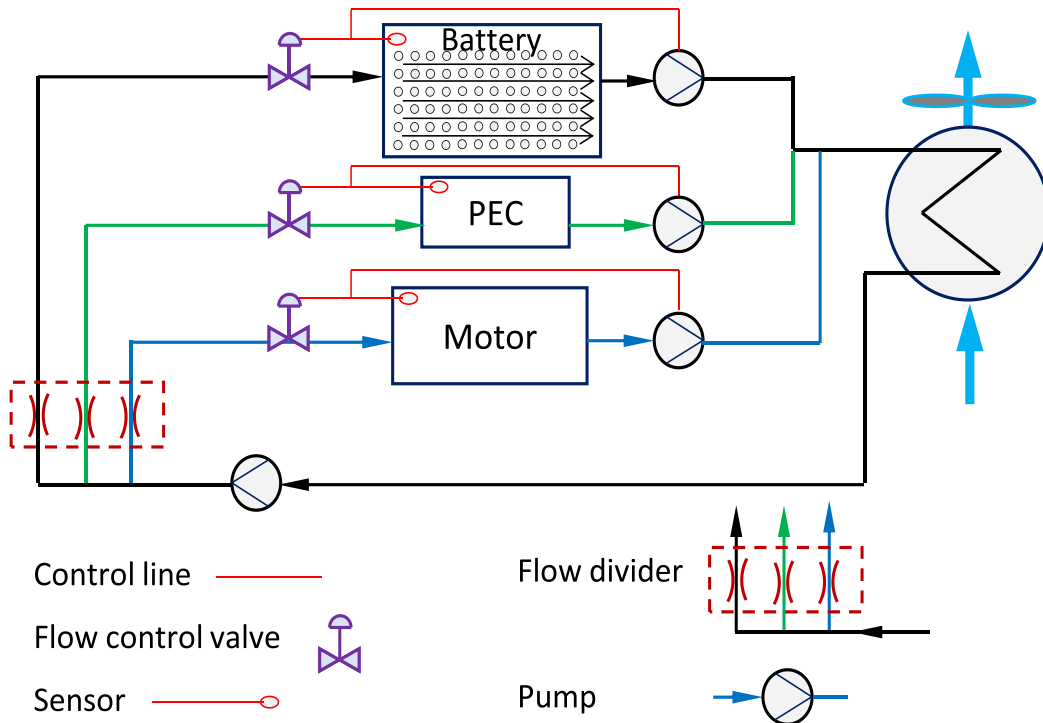
FIGURE 11. Proposed Pneumatic-Liquid Thermal Management System (PLTMS).

materials) cooling schemes are found to be more efficient. Some solutions have been proposed by the researchers to operate the battery at lower temperatures, which include pre-heat the battery to the operating temperature range by using hot air, liquid, phase change materials [29], [61], [62], [63], [64], [65] & sinusoidal alternating current or changing the chemical composition of the electrolyte with LiPF4 [66]. In the next section, a novel thermal management system is proposed based on air and liquid cooling methodology.

For the drive cycle presented in Figure 6 and the power demand in Figure 7, the change in temperature of the battery without any active thermal management system is shown in Figure 10.

B. PROPOSED THERMAL MANAGEMENT SYSTEM (TMS)

A novel hybrid Pneumatic-Liquid Thermal Management System (PLTMS) is proposed as shown in Figure 11, and the flowchart of the methodology of the proposed system is shown in Figure 12. The radiator supplies cold air to the main supply line which is then divided by the flow divider as per the requirement. The flow control value for the respective motor, power electronic converter and battery works on the differential operating temperature of the device. The hot air is exhausted out to the radiator for a closed loop operation to improve the efficiency of the system.

The proposed PLTMS is simulated, and the temperature control is shown in Figure 13. The stepwise algorithm of the proposed method is as follows:

STEP-1: Start

STEP-2: Monitor the temperature of the battery cells using temperature sensors

STEP-3: If the temperature is below the lower threshold, go to step 2

STEP-4: If the temperature is above the upper threshold, go to step 5

STEP-5: Activate the cooling system:

a. Turn on the pump to circulate liquid through the system
b. Turn on the fan to draw air through the heat exchanger

STEP-6: Transfer heat from the battery cells to the liquid:

a. The liquid flows through the heat exchanger, absorbing heat from the battery cells
b. The heat is transferred from the liquid to the air flowing through the heat exchanger

STEP-7: Dissipate the heat into the environment:

a. The hot air is expelled from the system through an exhaust port or duct
b. The cooled liquid returns to the battery cells to absorb more heat

STEP-8: Check if the temperature has reached the desired level:

a. If the temperature is below the upper threshold, go to step 2
b. If the temperature is still above the upper threshold, repeat steps 5-7

STEP-9: Deactivate the cooling system, and turn off the fan and pump
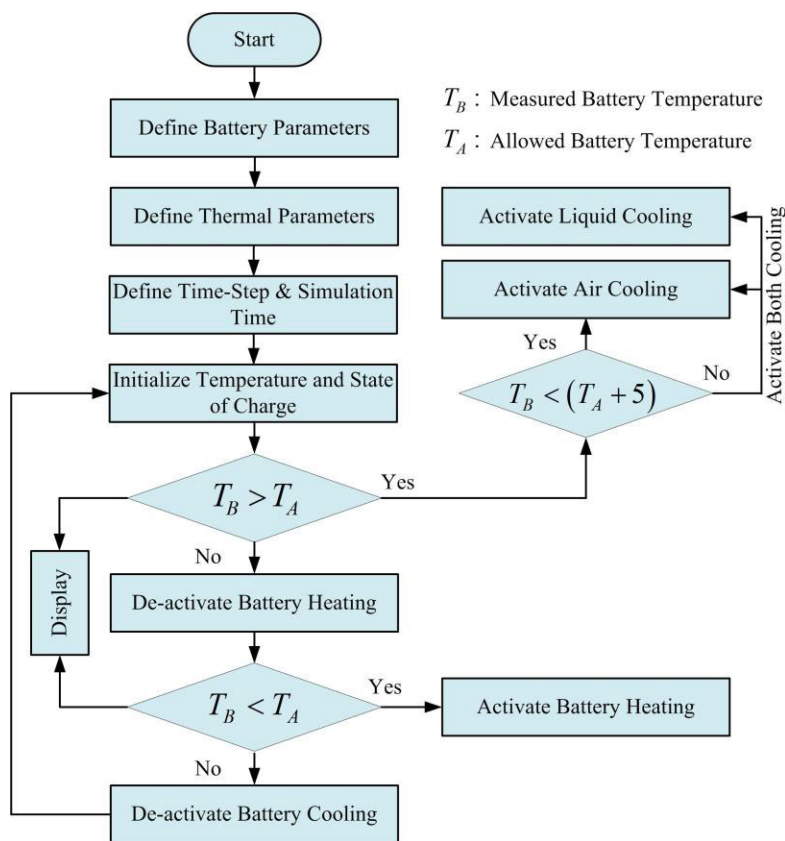
STEP-10: Stop

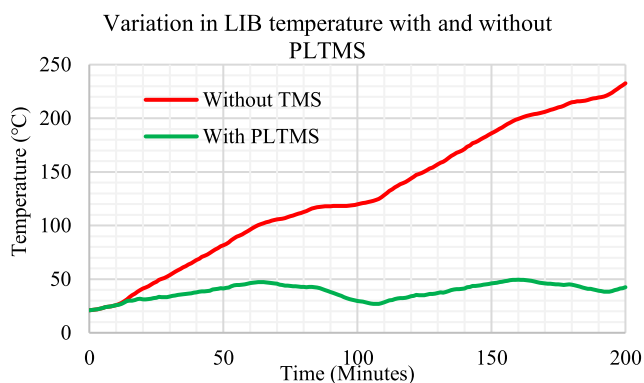**FIGURE 12.** Flowchart of the proposed TMS Scheme.

FIGURE 13. Temperature control of the battery with proposed PLTMS.

The authors have modelled the Pneumatic-Liquid Thermal Management Systems (PLTMS) in JavaScript and simulated the same using Python programming. The collected data points are plotted using the Microsoft Excel tool.

V. RESULTS AND DISCUSSION

Considering an EV with the total mass of 1350 kg (including payload), 175 / 65 R14 tyre with a diameter of 584 mm, and differential with 64 teeth on gear & 17 teeth on pinion giving a gear ratio of 3.765, the results are analyzed. Figure 14 presents the comparison of forces required to overcome rolling resistance, aerodynamic drag & gradient, and

total force at different speeds. The total force requirement ranges from 50 N to 220 N. The rolling resistance range from 61.66 to 132.9 N over the range of 0 to 120 kmph i.e. total variation is 71.28 N, and aerodynamic drag over the same range varies from 0 to 88.45 N i.e. total variation is 88.45 N. The influence of aerodynamic drag increases more rapidly as compared to other resistances. It can be inferred from Figure 14 that at starting, the rolling resistance is very high and as the vehicle velocity is increased, the drag force is more dominant. Similar conclusions can be made from Figure 15 and Figure 16 which outlines the torque requirements and energy requirements of the EV at different vehicle velocity. It is noted that the torque range varies from 18.1 to 64.65 N-m over the speed range from 0 to 120 kmph while the energy requirements range from 0 to 38.41 kW (51.51 hp). These results are comparable with the experimental results presented by Wang [67]. Maximum steady-state estimation of SOC and SOH can be achieved within 1% accuracy [68]. Accurate estimation of battery health [69] and maximum capacity [70] is necessary for reliability and optimal power utilization in EV.

The variation in the energy requirements with gradient is presented in Figure 17. It can be inferred from the figure that the power requirement is increasing with increase in the gradient and speed.

Table 7 summarizes the requirement of battery capacity at different speeds ranging from 60 kmph to 120 kmph for a
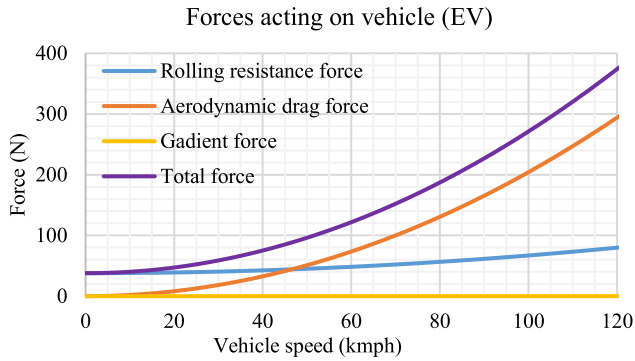
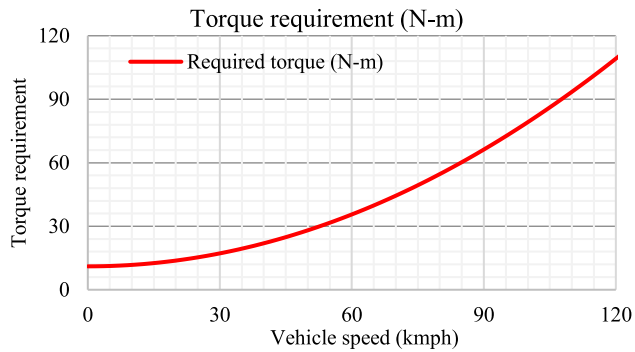**FIGURE 14.** Variation of different forces of an EV with variation on velocity.

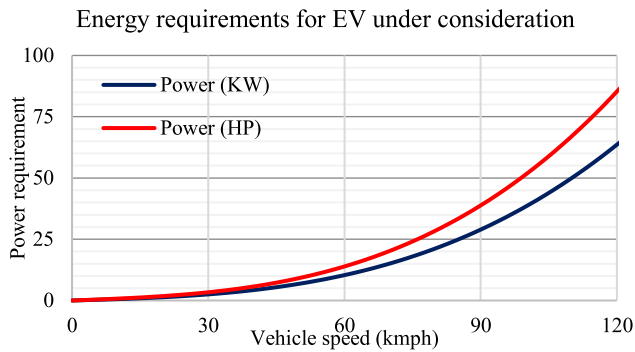**FIGURE 15.** Torque requirement of the EV under different vehicle velocities.

FIGURE 16. Energy requirements for EV under consideration.

driving range between 100 kms to 500 kms. The range goes from 18.11 kWh for 100 km range at 60 kmph to 560.1 kWh for 500 km range at 120 kmph. For instance, with a battery capacity of 60 kwh, the vehicle can provide a driving range of about 331 km at 60 kmph, 252 km at 70 kmph, 172 km at 80 kmph, and so on. It is clear from this discussion that vehicle velocity has a significant impact on the driving range of an EV.

VI. CONCLUSION

The mathematical model of a vehicle that includes rolling resistance, aerodynamic drag, and road gradient has been developed in the study. The simulation results for a vehicle with 1.6 m width and 1.5 m height and 1350 kg weight
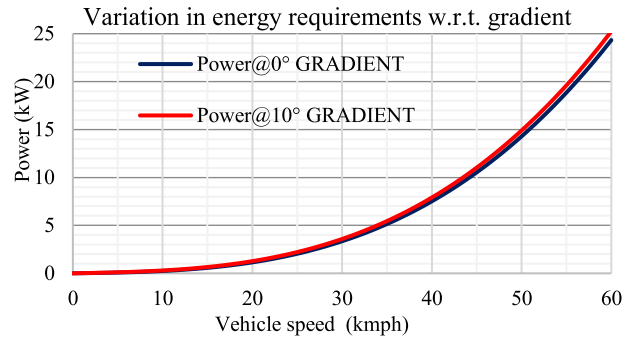

FIGURE 17. Variation in energy requirements for EV under consideration w.r.t. gradient.

TABLE 7. Battery capacity in kWh.

Speed (kmph)	Drive Range (in km)								
	100	150	200	250	300	350	400	450	500
60	18.11	27.16	36.21	45.26	54.32	63.37	72.42	81.48	90.53
70	23.75	35.63	47.51	59.39	71.26	83.14	95.02	106.9	118.8
80	34.46	51.7	68.93	86.16	103.4	120.6	137.9	155.1	172.3
90	48.23	72.35	96.46	120.6	144.7	168.8	192.9	217	241.2
100	65.47	98.2	130.9	163.7	196.4	229.1	261.9	294.6	327.3
110	86.59	129.9	173.2	216.5	259.8	303.1	346.4	389.7	433
120	112	168	224.1	280.1	336.1	392.1	448.1	504.1	560.1

with 35 PSI tyre pressure and 1.2 $\frac{kg}{m^3}$ air density at normal temperature and pressure are discussed. The results of the proposed model are in line with the available experimental drive cycle results. The model can also be simulated with varying meteorological conditions (varying air density, temperature & humidity), different driving behaviors of acceleration, deceleration, and braking inputs.

The rolling resistance varies from 61.66 N to 1 32.9 N in the speed range from 40 kmph to 120 kmph. The aerodynamic drag force becomes 10 times with a 10o change in the gradient irrespective of the vehicle velocity thereby following a non-linear path. The proposed model predicts that vehicle will consume 23 kW of the battery capacity in 200 minutes covering a distance of 64 km at a speed of 5.9 m/s, which is comparable with the available experimental results and is the most accurate prediction.

The following contributions are claimed in the present research:

- Extensive literature study to develop the model for prediction of driving force considering rolling resistance, aerodynamic drag, and gradient.
- Investigated the influence of tyre pressure and vehicle speed and temperature on rolling resistance.
- Initiated research towards the development of a precise mathematical model for the prediction of energy requirements to identify the power requirements for a road trip before traveling.

- Initiated a research perspective to give new scope to simulations of vehicle dynamics.
- Offer insights to develop an original thermal management system for the battery pack in general and the electric vehicle altogether.
- Proposed a Pneumatic Thermal Management System for maintaining the operating temperature of the battery, power electronic controller, and electric motor.

Although a novel mathematical model is proposed to understand the performance of electric vehicles under driving conditions, further initiatives are required to consider the gradient, temperature, tyre slip, and environmental factors in rolling resistance and aerodynamic drag. The authors also aim to further investigate the technological development in the area of forced air cooling with the following perspectives:

- Involving various artificial intelligence-based optimization algorithms to improve the performance of forced-air convection systems by reducing the amount of wasted energy and improving overall efficiency.
- Develop a hardware setup and drive cycle analysis of the proposed model.
- The influence of temperature on rolling resistance may be considered.
- By incorporating the proposed mathematical model into the digital twin, the current model will demonstrate the capability to fulfill the aforementioned tasks. This integration will allow for the effective implementation of the tyre pressure display and its associated functionalities, enabling EV users to optimize their vehicle's performance while ensuring safety and efficiency on the road.

ACKNOWLEDGMENT

REFERENCES
[1] K. Boriboonsomsin, M. J. Barth, W. Zhu, and A. Vu, "Eco-routing navigation system based on multisource historical and real-time traffic information," *IEEE Trans. Intell. Transp. Syst.*, vol. 13, no. 4, pp. 1694–1704, Dec. 2012.

[2] K. Brundell-Freij and E. Ericsson, "Influence of street characteristics, driver category and car performance on urban driving patterns," *Transp. Res. D, Transp. Environ.*, vol. 10, no. 3, pp. 213–229, May 2005.

[3] L. Raykin, M. J. Roorda, and H. L. MacLean, "Impacts of driving patterns on tank-to-wheel energy use of plug-in hybrid electric vehicles," *Transp. Res. D, Transp. Environ.*, vol. 17, no. 3, pp. 243–250, May 2012.

[4] C. Lorf, R. F. Martínez-Botas, D. A. Howey, L. Lytton, and B. Cussons, "Comparative analysis of the energy consumption and CO_2 emissions of 40 electric, plug-in hybrid electric, hybrid electric and internal combustion engine vehicles," *Transp. Res. D, Transp. Environ.*, vol. 23, pp. 12–19, Aug. 2013.

[5] C. Fiori, K. Ahn, and H. A. Rakha, "Power-based electric vehicle energy consumption model: Model development and validation," *Appl. Energy*, vol. 168, pp. 257–268, Apr. 2016.

[6] D. W. Wyatt, H. Li, and J. E. Tate, "The impact of road grade on carbon dioxide (CO_2) emission of a passenger vehicle in real-world driving," *Transp. Res. D, Transp. Environ.*, vol. 32, pp. 160–170, Oct. 2014.

[7] Z. Sun, P. Hao, X. J. Ban, and D. Yang, "Trajectory-based vehicle energy/emissions estimation for signalized arterials using mobile sensing data," *Transp. Res. D, Transp. Environ.*, vol. 34, pp. 27–40, Jan. 2015.

[8] J. Ejsmont, L. Goubert, G. Ronowski, and B. Świeczko-Żurek, "Ultra low noise poroelastic road surfaces," *Coatings*, vol. 6, no. 2, p. 18, Apr. 2016.

[9] Y. Sugiyama, M. Fukui, M. Kikuchi, K. Hasebe, A. Nakayama, K. Nishinari, S.-I. Tadaki, and S. Yukawa, "Traffic jams without bottlenecks—Experimental evidence for the physical mechanism of the formation of a jam," *New J. Phys.*, vol. 10, no. 3, Mar. 2008, Art. no. 033001.

[10] M. J. Schoenmakers, "Automated vehicles and infrastructure design: An insight into the implications of a dedicated lane for automated vehicles on the highway in The Netherlands," Dept. Build Environ., Eindhoven Univ. Technol., Eindhoven, The Netherlands, Tech. Rep., 2018.

[11] D. Gundana, R. A. Dollar, and A. Vahidi, "To merge early or late: Analysis of traffic flow and energy impact in a reduced lane scenario," in *Proc. 21st Int. Conf. Intell. Transp. Syst. (ITSC)*, Maui, HI, USA, Nov. 2018, pp. 525–530.

[12] I. Evtimov, R. Ivanov, and M. Sapundjiev, "Energy consumption of auxiliary systems of electric cars," in *Proc. MATEC Web Conf.*, Jan. 2017, p. 06002.

[13] K. Holmberg and A. Erdemir, "Influence of tribology on global energy consumption, costs and emissions," *Friction*, vol. 5, no. 3, pp. 263–284, Sep. 2017.

[14] Z. Gao, T. LaClair, S. Ou, S. Huff, G. Wu, P. Hao, K. Boriboonsomsin, and M. Barth, "Evaluation of electric vehicle component performance over eco-driving cycles," *Energy*, vol. 172, pp. 823–839, Apr. 2019.

[15] C. F. Kusuma, B. A. Budiman, and I. P. Nurprasetio, "Simulation method for extended-range electric vehicle battery state of charge and energy consumption simulation based on driving cycle," in *Proc. 6th Int. Conf. Electric Veh. Technol. (ICEVT)*, Bali, Indonasea, Nov. 2019, pp. 336–344.

[16] C. Lv, X. Hu, A. Sangiovanni-Vincentelli, Y. Li, C. M. Martinez, and D. Cao, "Driving-style-based codesign optimization of an automated electric vehicle: A cyber-physical system approach," *IEEE Trans. Ind. Electron.*, vol. 66, no. 4, pp. 2965–2975, Apr. 2019.

[17] B. Sharmila, K. Srinivasan, D. Devasena, S. Muthusamy, H. Panchal, R. A. Kumar, R. M. Kumari, K. K. Sadasivuni, and R. R. Shah, "Modelling and performance analysis of electric vehicle," *Int. J. Ambient Enegry*, vol. 43, no. 1, pp. 1–14, Jun. 2021.

[18] M. Mathankumar, B. Gunapriya, R. R. Guru, A. Singaravelan, and P. Sanjeevikumar, "AI and ML powered IoT applications for energy management in electric vehicles," *Wireless Pers. Commun.*, vol. 126, no. 2, pp. 1223–1239, Sep. 2022.

[19] F. Işıklı, A. Sürmen, and A. Gelen, "Modelling and performance analysis of an electric vehicle powered by a PEM fuel cell on new European driving cycle (NEDC)," *Arabian J. Sci. Eng.*, vol. 46, no. 8, pp. 7597–7609, Aug. 2021.

[20] I. Miri, A. Fotouhi, and N. Ewin, "Electric vehicle energy consumption modelling and estimation—A case study," *Int. J. Energy Res.*, vol. 45, no. 1, pp. 501–520, Jan. 2021.

[21] A. Skuza and R. S. Jurecki, "Analysis of factors affecting the energy consumption of an EV vehicle—A literature study," *IOP Conf. Ser., Mater. Sci. Eng.*, vol. 1247, no. 1, 2022, Art. no. 012001.

[22] M. D. Gennaro, E. Paffumi, G. Martini, U. Manfredi, H. Scholz, H. Lacher, H. Kuehnelt, and D. Simic, "Experimental investigation of the energy efficiency of an electric vehicle in different driving conditions," SAE 2014 World Congr. Exhib., SAE Int., USA, SAE Tech. Paper 2014-01-1817, 2014, doi: 10.4271/2014-01-1817.

[23] E. M. Szumska and R. S. Jurecki, "Parameters influencing on electric vehicle range," *Energies*, vol. 14, no. 16, p. 4821, Aug. 2021.

[24] Z. Teimoori and A. Yassine, "A review on intelligent energy management systems for future electric vehicle transportation," *Sustainability*, vol. 14, no. 21, p. 14100, Oct. 2022.

[25] Y. Ji, Y. Zhang, and C.-Y. Wang, "Li-ion cell operation at low temperatures," *J. Electrochem. Soc.*, vol. 160, no. 4, pp. 636–649, 2013.

[26] H.-C. A. Shiao, D. Chua, H.-P. Lin, S. Slane, and M. Salomon, "Low temperature electrolytes for Li-ion PVDF cells," *J. Power Sources*, vol. 87, nos. 1–2, pp. 167–173, Apr. 2000.

[27] S. S. Zhang, K. Xu, and T. R. Jow, "Low temperature performance of graphite electrode in Li-ion cells," *Electrochimica Acta*, vol. 48, no. 3, pp. 241–246, Dec. 2002.

[28] S. Panchal, J. Mcgrory, J. Kong, R. Fraser, M. Fowler, I. Dincer, and M. Agelin-Chaab, "Cycling degradation testing and analysis of a LiFePO4 battery at actual conditions," *Int. J. Energy Res.*, vol. 41, no. 15, pp. 2565–2575, Dec. 2017.

[29] J. Jaguemont, L. Boulon, and Y. Dubé, "A comprehensive review of lithium-ion batteries used in hybrid and electric vehicles at cold temperatures," *Appl. Energy*, vol. 164, pp. 99–114, Feb. 2016.

[30] T. M. Bandhauer, S. Garimella, and T. F. Fuller, "A critical review of thermal issues in lithium-ion batteries," *J. Electrochem. Soc.*, vol. 158, no. 3, p. R1, Jan. 2011.

[31] F. Adegbohun, A. von Jouanne, B. Phillips, E. Agamloh, and A. Yokochi, "High performance electric vehicle powertrain modeling, simulation and validation," *Energies*, vol. 14, no. 5, p. 1493, Mar. 2021.

[32] R. R. Kumar and K. Alok, "Adoption of electric vehicle: A literature review and prospects for sustainability," *J. Cleaner Prod.*, vol. 253, Apr. 2020, Art. no. 119911.

[33] M. Madziel and T. Campisi, "Energy consumption of electric vehicles: Analysis of selected parameters based on created database," *Energies*, vol. 16, no. 3, p. 1437, Feb. 2023.

[34] M. Al Halabi and A. Al Tarabsheh, "Modelling of electric vehicles using MATLAB/Simulink," SAE Int., USA, SAE Tech. Paper 2020-01-5086, 2020, doi: 10.4271/2020-01-5086.

[35] H. Wei, C. He, J. Li, and L. Zhao, "Online estimation of driving range for battery electric vehicles based on SOC-segmented actual driving cycle," *J. Energy Storage*, vol. 49, May 2022, Art. no. 104091.

[36] J. Hong, H. Zhang, and X. Xu, "Thermal fault prognosis of lithium-ion batteries in real-world electric vehicles using self-attention mechanism networks," *Appl. Thermal Eng.*, vol. 226, May 2023, Art. no. 120304.

[37] A. G. Olabi, H. M. Maghrabie, O. H. K. Adhari, E. T. Sayed, B. A. A. Yousef, T. Salameh, M. Kamil, and M. A. Abdelkareem, "Battery thermal management systems: Recent progress and challenges," *Int. J. Thermofluids*, vol. 15, Aug. 2022, Art. no. 100171.

[38] H. Jouhara, N. Khordehgah, N. Serey, S. Almahmoud, S. P. Lester, D. Machen, and L. Wrobel, "Applications and thermal management of rechargeable batteries for industrial applications," *Energy*, vol. 170, pp. 849–861, Mar. 2019.

[39] L. Feng, S. Zhou, Y. Li, Y. Wang, Q. Zhao, C. Luo, G. Wang, and K. Yan, "Experimental investigation of thermal and strain management for lithium-ion battery pack in heat pipe cooling," *J. Energy Storage*, vol. 16, pp. 84–92, Apr. 2018.

[40] R. Sabbah, R. Kizilel, J. R. Selman, and S. Al-Hallaj, "Active (air-cooled) vs. passive (phase change material) thermal management of high power lithium-ion packs: Limitation of temperature rise and uniformity of temperature distribution," *J. Power Sources*, vol. 182, no. 2, pp. 630–638, Aug. 2008.

[41] J. B. Heywood, *Internal Combustion Engine Fundamentals*. New York, NY, USA: McGraw-Hill, 1988.

[42] K. Das and S. Sharma, "Eco-routing navigation systems in electric vehicles: A comprehensive survey," in *Autonomous and Connected Heavy Vehicle Technology*, R. Krishnamurthi, A. Kumar, and S. S. Gill, Eds. London, U.K.: Academic, 2022, pp. 95–122.

[43] M. Untaru, G. Poţincu, A. Stoicescu, G. Pereş, and I. Tabacu, *Dinamica Autovehiculelor pe Roţi (Dynamics of Wheeled Motor Vehicles)*. Bucureşti, Romania: Editura Didacticǎ Şi Pedagogicǎ, 1981.

[44] *Stepwise Coastdown Methodology for Measuring Tyre Rolling Resistance*, Standard J2452, Society of Automotive Engineers Engineers, Warrendale, PA, USA, 1999.

[45] G. Genta and L. Morello, *The Automotive Chassis*, vol. 1, F. F. Ling, Ed. Cham, Switzerland: Springer, 2009.

[46] C. De Cauwer, J. Van Mierlo, and T. Coosemans, "Energy consumption prediction for electric vehicles based on real-world data," *Energies*, vol. 8, no. 8, pp. 8573–8593, Aug. 2015.

[47] I. M. Berry, "The effects of driving style and vehicle performance on the real-world fuel consumption of U.S. light-duty vehicles," Ph.D. dissertation, Massachusetts Inst. Technol., Cambridge, MA, USA, 2010.

[48] M. Ehsani, Y. Gao, S. E. Gay, and A. Emadi, *Modern Electric, Hybrid Electric, and Fuel Cell Vehicles: Fundamentals, Theory, and Design*. Boca Raton, FL, USA: CRC Press, 2005.

[49] S. Ma, M. Jiang, P. Tao, C. Song, J. Wu, J. Wang, T. Deng, and W. Shang, "Temperature effect and thermal impact in lithium-ion batteries: A review," *Prog. Natural Sci., Mater. Int.*, vol. 28, no. 6, pp. 653–666, Dec. 2018.

[50] N. Sato, "Thermal behavior analysis of nickel metal hydride batteries for electric vehicles," *JSAE Rev.*, vol. 21, no. 2, pp. 205–211, Apr. 2000.

[51] S. Wang, T. Wu, H. Xie, C. Li, J. Zhang, L. Jiang, and Q. Wang, "Effects of current and ambient temperature on thermal response of lithium ion battery," *Batteries*, vol. 8, no. 11, p. 203, Nov. 2022.

[52] X. Wang, Y. Zhang, H. Ni, S. Lv, F. Zhang, Y. Zhu, Y. Yuan, and Y. Deng, "Influence of different ambient temperatures on the discharge performance of square ternary lithium-ion batteries," *Energies*, vol. 15, no. 15, p. 5348, Jul. 2022.

[53] M. Steinstraeter, T. Heinrich, and M. Lienkamp, "Effect of low temperature on electric vehicle range," *World Electr. Vehicle J.*, vol. 12, no. 3, p. 115, Aug. 2021.

[54] D. Montone, "Temperature effects on motor performance," Haydon Kerk Motion Solutions, Pittman Motors, USA, Tech. Rep., 2017. Accessed: Jan. 22, 2023. [Online]. Available: https://www.haydonkerkpittman.com/learningzone/whitepapers/temperature-effects-on-dc-motor-performance

[55] A. R. M. Siddique, S. Mahmud, and B. V. Heyst, "A comprehensive review on a passive (phase change materials) and an active (thermoelectric cooler) battery thermal management system and their limitations," *J. Power Sources*, vol. 401, pp. 224–237, Oct. 2018.

[56] D. Zhao and G. Tan, "A review of thermoelectric cooling: Materials, modeling and applications," *Appl. Thermal Eng.*, vol. 66, nos. 1–2, pp. 15–24, May 2014.

[57] Y. Lyu, A. R. M. Siddique, S. H. Majid, M. Biglarbegian, S. A. Gadsden, and S. Mahmud, "Electric vehicle battery thermal management system with thermoelectric cooling," *Energy Rep.*, vol. 5, pp. 822–827, Nov. 2019.

[58] X. Li, Z. Zhong, J. Luo, Z. Wang, W. Yuan, G. Zhang, C. Yang, and C. Yang, "Experimental investigation on a thermoelectric cooler for thermal management of a lithium-ion battery module," *Int. J. Photoenergy*, vol. 2019, pp. 1–10, Feb. 2019.

[59] P. Qin, J. Sun, X. Yang, and Q. Wang, "Battery thermal management system based on the forced-air convection: A review," *eTransportation*, vol. 7, Feb. 2021, Art. no. 100097.

[60] J. Liu, Z. Wang, J. Gong, K. Liu, H. Wang, and L. Guo, "Experimental study of thermal runaway process of 18650 lithium-ion battery," *Materials*, vol. 10, no. 3, p. 230, Feb. 2017.

[61] J. Zhang, H. Ge, Z. Li, and Z. Ding, "Internal heating of lithium-ion batteries using alternating current based on the heat generation model in frequency domain," *J. Power Sources*, vol. 273, pp. 1030–1037, Jan. 2015.

[62] H.-S. Song, J.-B. Jeong, B.-H. Lee, D.-H. Shin, B.-H. Kim, T.-H. Kim, and H. Heo, "Experimental study on the effects of pre-heating a battery in a low-temperature environment," in *Proc. IEEE Vehicle Power Propuls. Conf. (VPPC)*, Oct. 2012, pp. 1198–1201.

[63] Y. Ji and C. Y. Wang, "Heating strategies for Li-ion batteries operated from subzero temperatures," *Electrochimica Acta*, vol. 107, pp. 664–674, Sep. 2013.

[64] C.-Y. Wang, G. Zhang, S. Ge, T. Xu, Y. Ji, X.-G. Yang, and Y. Leng, "Lithium-ion battery structure that self-heats at low temperatures," *Nature*, vol. 529, no. 7587, pp. 515–518, Jan. 2016.

[65] H. Ruan, J. Jiang, B. Sun, W. Zhang, W. Gao, L. Y. Wang, and Z. Ma, "A rapid low-temperature internal heating strategy with optimal frequency based on constant polarization voltage for lithium-ion batteries," *Appl. Energy*, vol. 177, pp. 771–782, Sep. 2016.

[66] S. S. Zhang, K. Xu, and T. R. Jow, "A new approach toward improved low temperature performance of Li-ion battery," *Electrochem. Commun.*, vol. 4, no. 11, pp. 928–932, Nov. 2002.

[67] J. Wang, "Battery electric vehicle energy consumption modelling, testing and prediction: A practical case study," Ph.D. dissertation, Dept. Mech. Eng., Technische Universiteit Eindhoven, Eindhoven, The Netherlands, 2016.

[68] X. Hu, H. Yuan, C. Zou, Z. Li, and L. Zhang, "Co-estimation of state of charge and state of health for lithium-ion batteries based on fractional-order calculus," *IEEE Trans. Veh. Technol.*, vol. 67, no. 11, pp. 10319–10329, Nov. 2018.

[69] Y. Zhang, T. Wik, J. Bergström, and C. Zou, "State of health estimation for lithium-ion batteries under arbitrary usage using data-driven multi-model fusion," *IEEE Trans. Transport. Electrific.*, early access, Apr. 14, 2023, doi: 10.1109/TTE.2023.3267124.

[70] K. Peng, Z. Deng, Z. Bao, and X. Hu, "Data-driven battery capacity estimation based on partial discharging capacity curve for lithium-ion batteries," *J. Energy Storage*, vol. 67, Sep. 2023, Art. no. 107549.

• • •